*Progress In Electromagnetics Research M, Vol. 94, 41–49, 2020*

# CPW-Fed All-Metallic Vivaldi Antennas with Pattern Diversity for Millimeter Wave 5G Access Points

**Gulur S. Karthikeya*, Mahesh P. Abegaonkar, and Shiban K. Koul**

**Abstract**—A coplanar waveguide (CPW) fed uniplanar all-metallic antenna is proposed for mmWave 5G access points. The antenna has an impedance bandwidth from 26 to 30 GHz with a corresponding end-fire gain of 8 dBi at 28 GHz. The effective radiating volume is $0.0031\lambda_0^3$ indicating a high gain yield for minimal physical footprint. The radiation efficiency is 99.5%, and the losses are primarily due to finite conductivity of copper. The pattern integrity is high across the band with cross-polarization level below 30 dB, due to lack of electrically thick dielectric substrate. Industry standard low-cost chemical etching technique is used for fabrication of the prototype. A compact, co-polarized stacked beam switching module is also proposed for wide angular coverage with three-ports. This module houses the proposed all-metallic antennas for beam switchability. A customized 3D-printed scaffolding using polylactic acid (PLA) is designed to house the proposed antennas. The antenna module has a wide angular coverage of $\pm 50^\circ$. Since the proposed antenna has high radiation efficiency with high gain for minimal physical footprint, it could be a potential solution for mmWave 5G access points. Detailed simulated and measured results are presented with technical justification.

## 1. INTRODUCTION

The humongous growth in bandwidth hungry applications on smartphone ecosystem has provoked researchers to design future cellular networks at higher carrier frequencies. The 28 GHz band is one of the most advertised candidates for future 5G networks [1]. This would mean that the hardware must be built to cater for the 28 GHz carrier frequency on both the mobile devices and base stations or access points [2].

The primary issue with designing antenna systems at such high frequencies is the free space path loss which increases with the carrier frequency indicating that the path loss alone would be at least 20–30 dB higher than its commercial 4G or WiFi counterpart. The testing campaign has also demonstrated that the path loss due to common construction materials such as bricks, concrete, and glass windows is of the order of 30–40 dB [1] which has provoked experts to opine that a heterogeneous network of indoor and outdoor networks might be an apt solution for this problem. In other words, the base stations would be pumping power with pencil beams to the respective mobile devices in the outdoor network, and moderately high gain antennas would be used with access points in the indoor networks.

In both the cases, high gain antennas must be integrated on both the mobile device and access point to mitigate the effect of high free space path loss at least in principle. The design of a multi-beam antenna module for access points to be used in the context of indoor access points is the theme of this paper. The antennas to be designed for access points must have high radiation efficiency, minimal electrical footprint, high gain, and wide angular coverage. One of the most popular approaches to achieve these objectives is to design a phased array, which leads to increased physical footprint and complexity in beam control [3–9]. In addition to this, separate phase shifter controller networks have

*Received 20 May 2020, Accepted 23 June 2020, Scheduled 5 July 2020*
* Corresponding author: Gulur Sadananda Karthikeya (karthikeyaglr@gmail.com).
The authors are with the Centre for Applied Research in Electronics (CARE), IIT Delhi, New Delhi, India.

to be designed. The number of antennas and beams required would be decided by the user density in the local geography.

A simpler solution would be to design a multi-beam antenna module with a simple high isolation switch to control the beam. Phased arrays would also suffer from scanning loss close to 2 dB, when the primary radiating beam is scanned at 30° with respect to the boresight radiating axis, as evident in [3, 4, 6]. Conventional microstrip based printed circuit board (PCB) based antennas would encounter dielectric loss due to finite dielectric loss tangent of the substrate [3]. It must also be observed that the presence of dielectric would support surface wave modes and hence leading to spurious radiation specifically from the dielectric. The dielectric based end-fire antennas designed with PCB manufacturing would also suffer from high radiation due to cross-polarization levels as the radiating arms would be designed in separate radiating planes [3, 6]. One of the strategies to achieve high radiation efficiency is to design antennas without dielectric. Horn antennas with metal 3D-printing have been reported in [10, 11], and this procedure requires precision 3D-printing with stringent requirements on the surface resolution of the metal finish. Even though the all-metallic 3D-printed antennas are lighter in weight and exhibit high radiation efficiency, it is non-planar and bulky to be integrated into commercial access points. All-metallic antennas are commonly designed for low frequency radars as illustrated in [12, 13]. The antennas typically designed for radars have aluminium fabricated using wire-EDM (Electrical discharge machining) technology. The other method to reduce dielectric loss is to design waveguide feed such as a printed ridge gap waveguide as illustrated in [14], and it requires precision manufacturing. The design process is complicated as well. The cross-pol radiation level could be reduced by designing a co-planar stripline (CPS) feed such as [15], but this antenna requires additional impedance transformer when being fed by a balanced feed. Also, CPS feeding does not necessarily reduce dielectric loss since the design is a typical PCB based design built upon a typical dielectric with non-zero dielectric loss tangent.

Electromagnetic band gap (EBG) structures could be incorporated with the feeding transmission lines for mitigation of surface waves [16, 17], and these antennas also require precise manufacturing in addition to complex assembly process. In order to increase the gain of traveling wave antennas such as tapered slot antenna, the physical aperture could be elongated, or the radiating aperture could be integrated with phase-correcting sub-wavelength metamaterial unit cells or electrically large dielectric lens [18, 19]. The concept of metamaterial integration would definitely increase the gain of the antenna at the cost of increased dielectric loss and a compromise in the cross-pol radiation. Conventional stripline feeding could also be used for reducing radiation losses due to feeding, but the dielectric loss would increase due to elongated feeding design. Also, the stripline based antennas need multilayer PCB assembly [20]. Hence, an all-metallic tapered slot antenna with CPW feeding, fabricated by industry standard low-cost chemical etching method, is investigated in this paper.

Pattern diversity architectures are necessary to achieve wide angular coverage. Access points need compact design with beam switch ability as demonstrated in designs such as [21–26]. These designs suffer from relatively low radiation efficiency and high cross-pol levels. Hence, a co-polarized stacked design is investigated to achieve pattern diversity with wide angle coverage.

## 2. ANTENNA DESIGN

Microstrip feeding would incorporate a dielectric and hence leads to losses. The same problem is observed with aperture coupling or proximity feed. In order to design a planar all-metallic antenna, CPW feeding technique is the preferred choice. However, designing a CPW feed is challenging at millimeter wave frequencies due to the inherent issues in realizing the dimensions necessary for matching the antenna with the 50 Ω of the port. For instance, in order to realize a 50 Ω CPW feeding line the trace width has to be 2 mm with a gap of 20 µm. These dimensions would be impossible to achieve with standard chemical etching whose minimum resolution is only 50 µm. Hence, a feeding line of 78 Ω is designed which has a trace width of 2 mm and a gap of 0.2 mm. The arms of the planar traveling wave antenna would be based on CPS (Coplanar Stripline) which has a high impedance of 168 Ω. In order to match the characteristic impedance of 78 Ω of the CPW feed with 168 Ω of CPS lines of the radiator, a balun is introduced in between these structures which doubles up as an impedance transformer. The proposed CPW-fed planar all-metallic antenna is depicted in Fig. 1(a). The inset of Fig. 1(a) clearly indicates

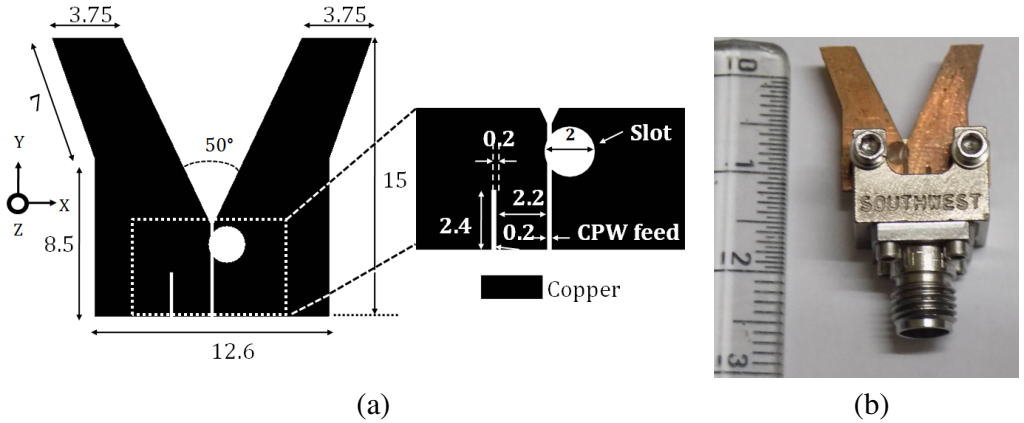


**Figure 1.** Proposed all-metallic planar antenna. (a) Schematic of the all-metallic antenna (units: mm). (b) Photograph of the fabricated prototype.

the feeding structure of the antenna. The fabricated prototype is shown in Fig. 1(b). The CPW feed is optimized for the 50 Ω port impedance of the end-launch connector. The connector type is 2.92 mm southwest end-launch connector which works up to 40 GHz. The width of the primary trace of the CPW feeding line is chosen to accommodate the grounding screws of the connector and to maintain feasible transition to the radiating aperture. The width of the overall antenna at the feeding plane is designed to incorporate the connector, and the feeding width otherwise could be smaller. A balun is designed for impedance matching between the CPW feed line and radiating aperture. Tapering of the antenna is optimized for a gain of 8 dBi in the end-fire. A copper sheet of 80 µm thickness is used for fabrication using industry standard chemical etching. Thinner copper sheets would be fragile to handle during chemical etching, and thicker Copper sheets would consume more time and chemicals for fabrication. In addition, thicker sheets beyond 500 µm would be difficult to clamp with the end-launch connector. A 3D-printed dielectric spacer of thickness 500 µm is used at the feed to prevent shorting of the trace pin and the clamping plate of the end-launch connector. This concept is unique to the class of planar all-metallic antennas.

Figure 2(a) illustrates the $E$-fields in the $XY$-plane for the proposed all-metallic antenna at 28 and 30 GHz. The transmission line mode and travelling wave modes are distinctly visible in the illustration. The balun acts as an impedance transformer from CPW to CPS (coplanar stripline). The variation of the input reflection coefficient with respect to the radius of the balun is shown in Fig. 2(b), and the parametric analysis clearly indicates that the radius of the balun is a key parameter to control the impedance matching. When the circular slot is 0.5 mm, the CPW feed is poorly matched with the CPS antenna. On the other hand, the antenna is detuned to 29 GHz when the slot radius is 1.5 mm. Hence, the optimal radius is 1 mm. The input reflection coefficient of the proposed element is depicted in Fig. 2(c). The simulated 10 dB impedance bandwidth is from 26–30 GHz translating to 14.3%, but the measured impedance bandwidth is 27.2–31 GHz translating to 13%. The effects of electrically large connector is not accounted for in full-wave simulations in Ansys HFSS. The discrepancy between simulation and measured results is due to the lack of soldering at the transition of the antenna with the connector. It must also be noted that the spacer included in the measurements to avoid shorting of the trace pin and the grounding plate of the end-launch connector has created deviation from the simulated curve. It is well known that the characteristic impedance of the end-launch connector is close to 50 Ω up to and including 40 GHz. The deviation might also be due to the bending stress encountered at the transition between the trace pin of the connector and the antenna, due to multiple mating cycles of the connector. The $E$-plane ($XY$ plane) radiation patterns are shown in Fig. 3(a) for 28 and 30 GHz, and the beamwidth is $36° \pm 0.5°$, indicating high pattern integrity across the band. The $H$-plane ($YZ$ plane) patterns are illustrated in Fig. 3(b). The front to back ratio is more than 10 dB in spite of the electrically small ground.

The cross-polarization level is less than 30 dB across the band, in the $E$-plane as the radiator is

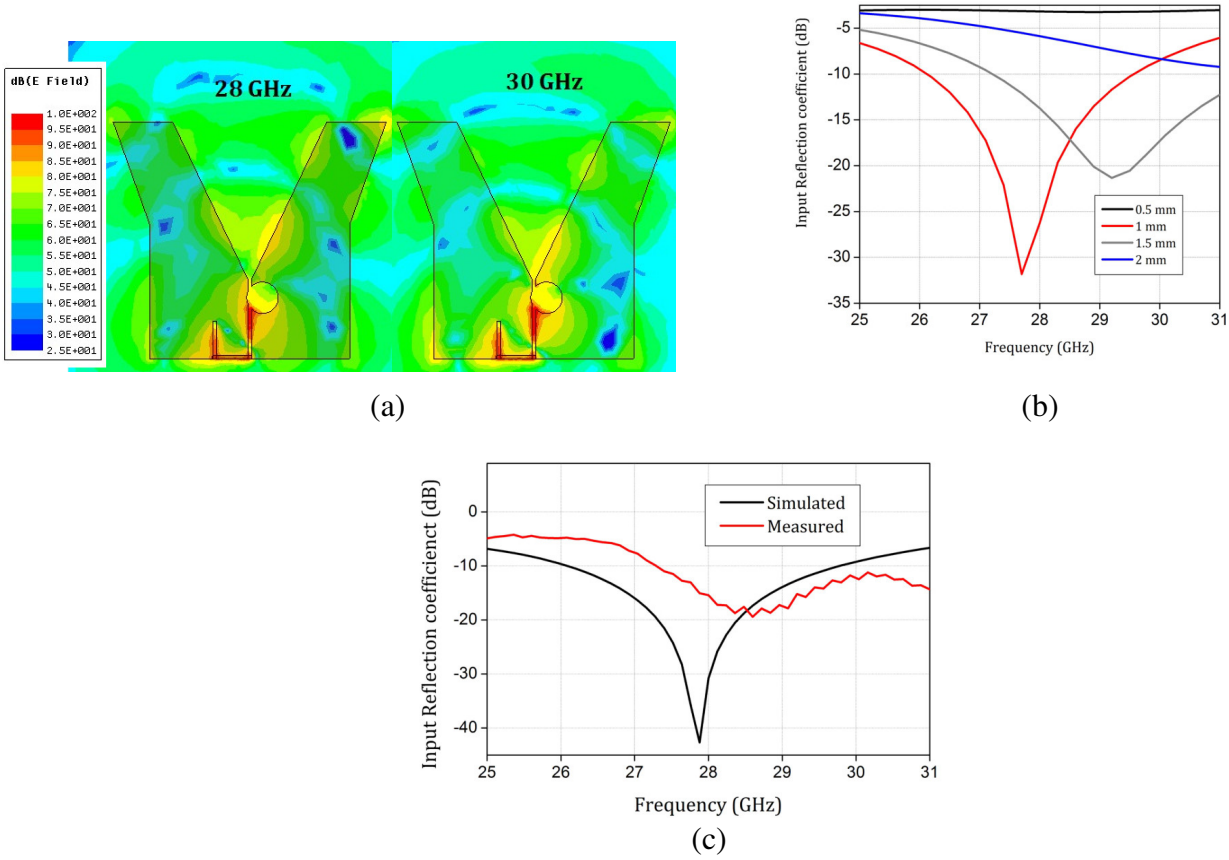


**Figure 2.** (a) *E*-fields at 28 and 30 GHz. (b) Parametric analysis of the antenna. (c) Input reflection coefficients of the proposed all-metallic antenna.

coplanar with minimal radiation in the orthogonal polarization. The forward gain is close to 8 dBi at 28 GHz indicating high gain yield for minimal physical footprint. The gain variation is within 1 dB across the band as observed in Fig. 4. The measurement is done using the gain transfer method. The discrepancy between the simulated and measured results is primarily due to the alignment error during measurement. Customized stands with laser aligners would improve the measurement results. The dielectric based antenna for the same physical dimensions would yield a gain of close to 7.5 dBi. It must also be noted that the dielectric based antenna has a limitation on the power handling capability due to the inherent dielectric breakdown. On the other hand, all-metallic design has a relatively higher power handling capability proving to be a useful design feature for access points. The typical power handling requirement for indoor access points would be in the range of +30 dBm to +50 dBm. A comparison of simulated radiation efficiency of the proposed all-metallic antenna and conventional PCB antenna based on a Nelco NY9220 substrate of 500 µm thickness and dielectric loss tangent of 0.0009 is depicted in Fig. 5. The proposed antenna has a radiation efficiency of 99.5%, and the only loss encountered in the proposed antenna is the finite conductivity of copper. The other alternate strategy for radiation efficiency enhancement is to use electrically thinner substrate, which increases the cost of manufacturing.

In order to achieve beam switching for wide angular coverage, a compact co-polarized stacked multi-beam module is proposed. Conventional phased arrays designed for beam scanning suffers from scanning loss, hence degrading the beam integrity during scanning [3]. A co-polarized stacking beam switching module is proposed as observed in Fig. 6(a), and the fabricated prototype is shown in Fig. 6(b). The distance between the antenna elements is maintained at 10 mm to accommodate the end-launch connector. In addition to this, if the antenna elements are mounted closer then the central element's pattern will be distorted due to waveguiding effect of the top and bottom metallic

antennas. A customized 3D-printed scaffolding was designed using polylactic acid (PLA) material, with a dielectric constant of 2.75 and a loss tangent of 0.015. The scaffolding does not influence the radiation characteristics of the mounted antennas. Additional scaffoldings were designed for holding the bulky connector, and the radiating beams were measured one port at a time. The orientation of the individual antennas is to maintain a reasonable angular coverage. The angular coverage of the beam switching module is $\pm 50^{\circ}$ as seen in Fig. 7(a). The simulated mutual coupling is less than 25 dB across the band and ports as seen in Fig. 7(b), primarily due to low cross-polarization levels of individual radiators and its associated angular orientation. It is assumed that a high isolation SP3T switch will switch the antennas depending on the users required in that specific angular zone.

Table 1 illustrates the advantages of the proposed element compared to previously reported designs. Here, effective radiating volume is primarily the ratio of the physical volume of the antenna excluding the feed portion to the cube of the operating wavelength in free space. This metric gives an insight into actual electrical size of the radiating portion of the antenna. The proposed design yields a uniplanar antenna with simplified feeding technique and high radiation efficiency. Even though the effective

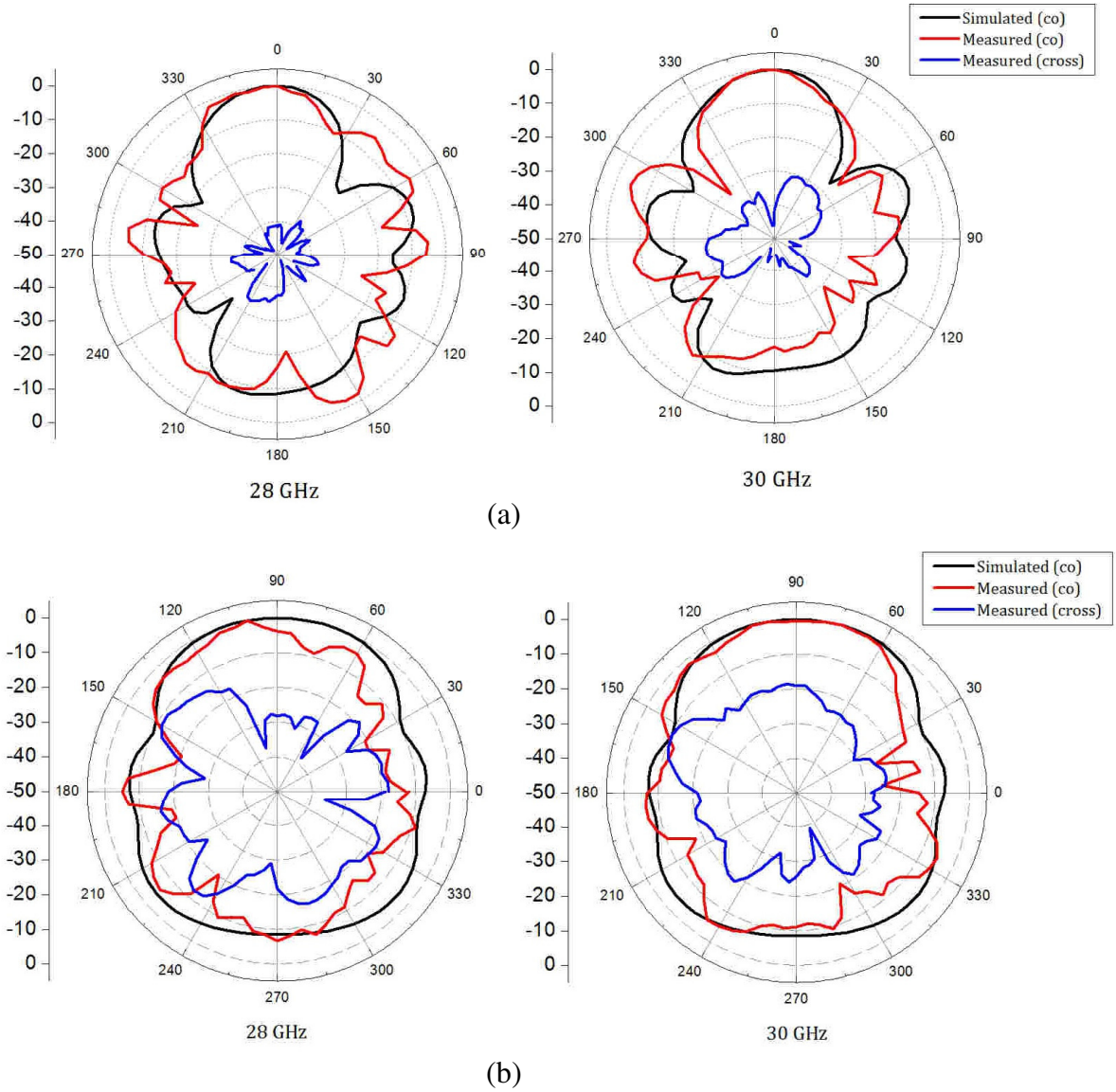


**Figure 3.** Radiation patterns of the all-metallic antenna (a) $E$-plane, (b) $H$-plane.

radiating volume of [3] is low, the gain yield for single element is lower. The insertion loss is minimal in [4] due to SIW feeding at the cost of increased physical footprint. Various PCB based antennas have either high cross-pol or higher physical footprint than the proposed element [5–13]. The printed ridge gap waveguide feeding in [14] also has minimal loss in the dielectric, but the multilayer structure increases fabrication cost and the time to design the antenna. The coplanar strip line feed presented in [15] requires additional baluns or impedance transformers from active circuits for feeding the antenna. Even high frequency designs have higher effective radiating volume than the proposed antenna [18–23].

**Table 1.** Comparison against reported articles.

| References | F | G | ERV | Feed | Type | Material | Beam Switching |
|---|---|---|---|---|---|---|---|
| [3] | 28 | 5.5 | 0.0062 | MS[1] | PCB | RT Duroid 5880 | ±45° |
| [4] | 28 | 9 | 0.138 | SIW[2] | All-metallic | RT Duroid 5880 | ±35° |
| [5] | 2.5 | 6.1 | 0.116 | CX[3] | PCB | FR4 | -NA- |
| [6] | 28 | 6 | 0.006 | MS[1] | Multilayer PCB | Taconic RF-35 | ±45° |
| [7] | 60 | 20 | 68.64 | MS[1] | PCB + dielectric lens | Rogers RO4003 | ±30° |
| [8] | 28 | 12 | 0.027 | CX[3] | PCB | RT Duroid 5880 | -NA- |
| [9] | 28 | 5 | 0.005 | CX[3] | Multilayer PCB | ISOLA IS300MD | -NA- |
| [14] | 30 | 7.5 | 0.114 | PRG[4] | PCB | RO3003 | -NA- |
| [15] | 24 | 10 | 0.018 | CPS[5] | PCB | RT Duroid 5880 | -NA- |
| [18] | 10 | 14 | 0.04 | MS[1] | PCB | F4B | -NA- |
| [19] | 64 | 11 | 0.08 | MS[1] | PCB | Ferro A6S | -NA- |
| [21] | 16 | 8.5 | 0.14 | MS[1] | PCB | FR4 | 0°, 180°, ±90° |
| [22] | 5.8 | 4 | 0.016 | CX[3] | PCB | FR4 | 0°, 180°, 90° |
| [23] | 28 | 11 | 0.05 | MS[1] | PCB | Neltec NY9220 | ±30° |
| **Proposed** | **28** | **7.6** | **0.0031** | **CPW** | **All-metallic** | **Copper** | **±50°** |

*$F$ = Centre frequency (GHz), $G$ = Gain (dBi), ERV = Effective Radiating volume ($\lambda_0^3$)
[1]Microstrip, [2]Substrate Integrated Waveguide, [3]Coaxial feed [4]Printed Ridge gap, [5]Coplanar Stripline

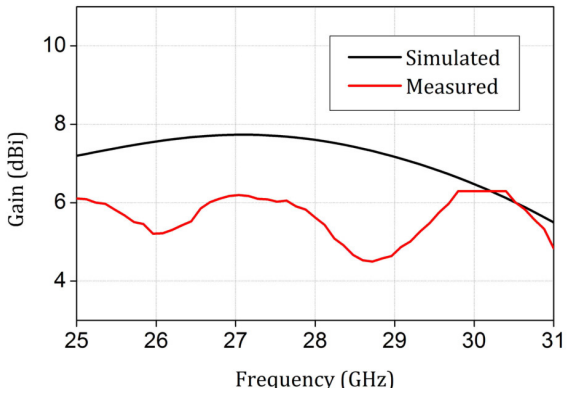


**Figure 4.** Forward gain of the proposed antenna.

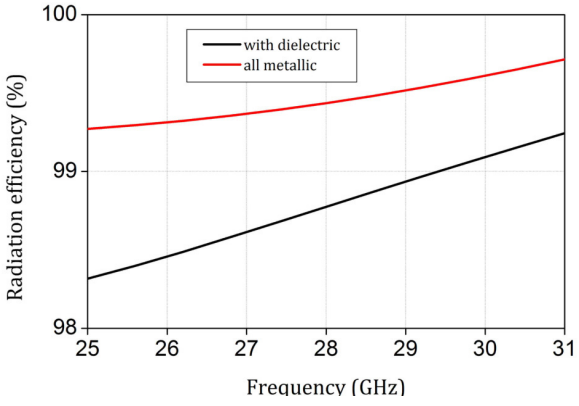


**Figure 5.** Radiation efficiency of proposed antenna.

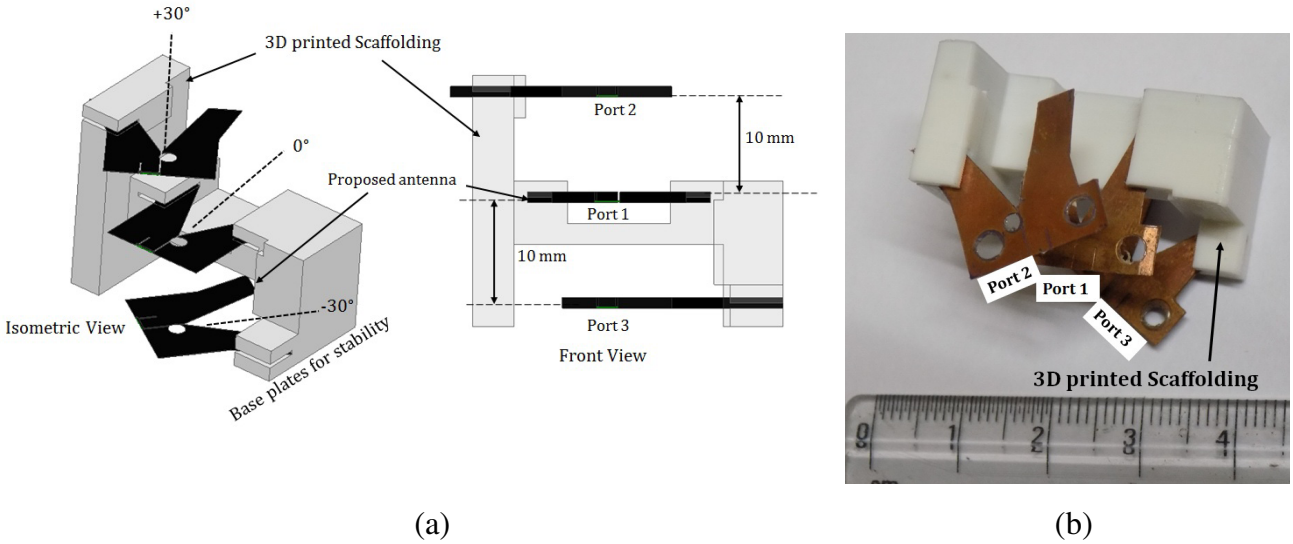


**Figure 6.** Beam switching module. (a) Schematics of the module (units: mm). (b) Photograph of the fabricated module (isometric view).

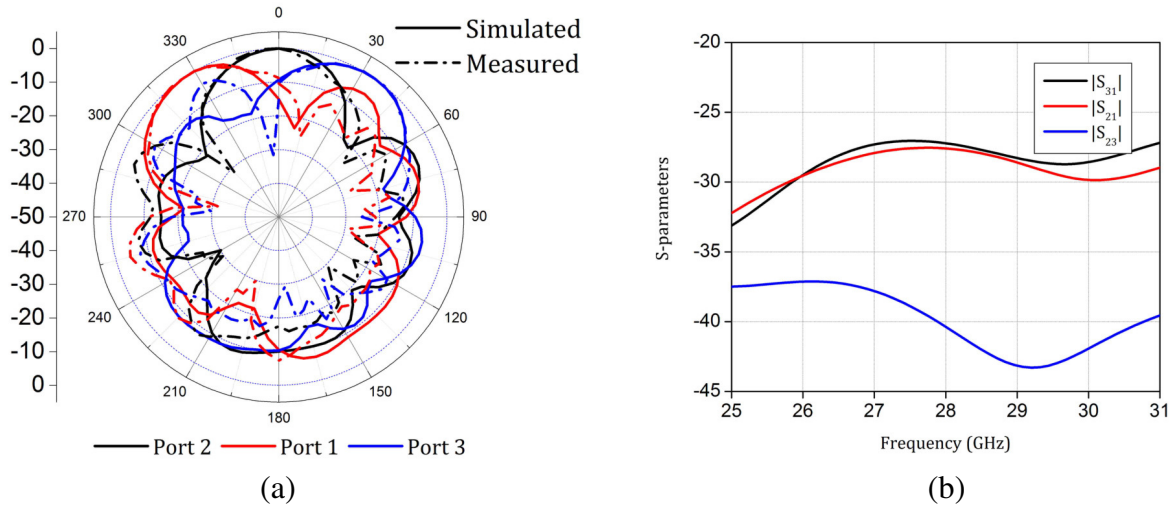


**Figure 7.** (a) Radiation pattern of the module at 28 GHz. (b) Mutual coupling of the stacked module.

## 3. CONCLUSION

A CPW-fed all-metallic antenna operating in the 28 GHz band with an impedance bandwidth of 14.3% is proposed. The proposed antenna has a forward end-fire gain of 7.6 dBi for an effective radiating volume of $0.0031\lambda_0^3$. A co-polarized stacked beam switching module has also been proposed. The proposed antenna and the beam switching module could be a useful candidate for future millimeter wave 5G access points.

## REFERENCES

1. Rappaport, T. S., et al., "Millimeter wave mobile communications for 5G cellular: It will work!," *IEEE Access*, Vol. 1, 335–349, 2013.

2. Hong, W., K. Baek, Y. Lee, Y. Kim, and S. Ko, "Study and prototyping of practically large-scale mmWave antenna systems for 5G cellular devices," *IEEE Communications Magazine*, Vol. 52, No. 9, 63–69, Sep. 2014.
3. Ta, S. X., H. Choo, and I. Park, "Broadband printed-dipole antenna and its arrays for 5G applications," *IEEE Antennas and Wireless Propagation Letters*, Vol. 16, 2183–2186, 2017.
4. Yang, B., Z. Yu, Y. Dong, J. Zhou, and W. Hong, "Compact tapered slot antenna array for 5G millimeter-wave massive MIMO systems," *IEEE Transactions on Antennas and Propagation*, Vol. 65, No. 12, 6721–6727, Dec. 2017.
5. Liu, F., J. Guo, L. Zhao, X. Shen, and Y. Yin, "A meta-surface decoupling method for two linear polarized antenna array in sub-6 GHz base station applications," *IEEE Access*, Vol. 7, 2759–2768, 2019.
6. Shim, J., J. Go, and J. Chung, "A 1-D tightly coupled dipole array for broadband mmWave communication," *IEEE Access*, Vol. 7, 8258–8265, 2019.
7. Briqech, Z., A. Sebak, and T. A. Denidni, "Wide-scan MSC-AFTSA array-fed grooved spherical lens antenna for millimeter-wave MIMO applications," *IEEE Transactions on Antennas and Propagation*, Vol. 64, No. 7, 2971–2980, Jul. 2016.
8. Ikram, M., E. A. Abbas, N. Nguyen-Trong, K. H. Sayidmarie, and A. Abbosh, "Integrated frequency-reconfigurable slot antenna and connected slot antenna array for 4G and 5G mobile handsets," *IEEE Transactions on Antennas and Propagation*, Vol. 67, No. 12, 7225–7233, Dec. 2019.
9. Hwang, I., B. Ahn, S. Chae, J. Yu, and W. Lee, "Quasi-Yagi antenna array with modified folded dipole driver for mmWave 5G cellular devices," *IEEE Antennas and Wireless Propagation Letters*, Vol. 18, No. 5, 971–975, May 2019.
10. Garcia, C. R., R. C. Rumpf, H. H. Tsang, and J. H. Barton, "Effects of extreme surface roughness on 3D printed horn antenna," *Electronics Letters*, Vol. 49, No. 12, 734–736, Jun. 6, 2013.
11. Tak, J., D.-G. Kang, and J. Choi, "A lightweight waveguide horn antenna made via 3D printing and conductive spray coating," *Microw. Opt. Technol. Lett.*, Vol. 59, 727–729, 2017.
12. Kindt, R. W. and W. R. Pickles, "Ultrawideband all-metal flared-notch array radiator," *IEEE Transactions on Antennas and Propagation*, Vol. 58, No. 11, 3568–3575, Nov. 2010.
13. Kedar, A., "Dielectric free wide scan UWB low cross-pol metallic Vivaldi antenna for active phased array radars," *IETE Journal of Research*, 1–9, May 30, 2019.
14. Sorkherizi, M. S., A. Dadgarpour, and A. A. Kishk, "Planar high-efficiency antenna array using new printed ridge gap waveguide technology," *IEEE Transactions on Antennas and Propagation*, Vol. 65, No. 7, 3772–3776, Jul. 2017.
15. Alhalabi, R. A. and G. M. Rebeiz, "Differentially-fed millimeter-wave Yagi-Uda antennas with folded dipole feed," *IEEE Transactions on Antennas and Propagation*, Vol. 58, No. 3, 966–969, Mar. 2010.
16. Cheype, C., C. Serier, M. Thevenot, T. Monediere, A. Reineix, and B. Jecko, "An electromagnetic bandgap resonator antenna," *IEEE Transactions on Antennas and Propagation*, Vol. 50, No. 9, 1285–1290, Sep. 2002.
17. de Maagt, P., R. Gonzalo, Y. C. Vardaxoglou, and J. Baracco, "Electromagnetic bandgap antennas and components for microwave and (Sub)millimeter wave applications," *IEEE Transactions on Antennas and Propagation*, Vol. 51, No. 10, 2667–2677, Oct. 2003.
18. Zhou, B., H. Li, X. Zou, and T.-J. Cui, "Broadband and high-gain planar Vivaldi antennas based on inhomogeneous anisotropic zero-index metamaterials," *Progress In Electromagnetics Research*, Vol. 120, 235–247, 2011.
19. Sun, M., Z. N. Chen, and X. Qing, "Gain enhancement of 60-GHz antipodal tapered slot antenna using zero-index metamaterial," *IEEE Transactions on Antennas and Propagation*, Vol. 61, No. 4, 1741–1746, Apr. 2013.
20. Lewis, L., M. Fassett, and J. Hunt, "A broadband stripline array element," *1974 Antennas and Propagation Society International Symposium*, 335–337, Atlanta, GA, USA, 1974.

21. Reddy, G. S., A. Kamma, S. Kharche, J. Mukherjee, and S. K. Mishra, "Cross-configured directional UWB antennas for multidirectional pattern diversity characteristics," *IEEE Transactions on Antennas and Propagation*, Vol. 63, No. 2, 853–858, Feb. 2015.
22. Sharma, Y., D. Sarkar, K. Saurav, and K. V. Srivastava, "Three-element MIMO antenna system with pattern and polarization diversity for WLAN applications," *IEEE Antennas and Wireless Propagation Letters*, Vol. 16, 1163–1166, 2017.
23. Wani, Z., M. P. Abegaonkar, and S. K. Koul, "Millimeter wave antenna with wide scan angle radiation characteristics for MIMO applications," *Int. J. RF Microw. Comput. Aided Eng.*, e21564, 2018.
24. Hasan, M. N., S. Bashir, S. Chu, "Dual band omnidirectional millimeter wave antenna for 5G communications," *Journal of Electromagnetic Waves and Applications*, Vol. 33, No. 12, 1581–1590, 2019.
25. Fernandez-Martinez, P., S. Martin-Anton, and D. Segovia-Vargas, "Design of a wideband Vivaldi antenna for 5G base stations," *2019 IEEE International Symposium on Antennas and Propagation and USNC-URSI Radio Science Meeting*, 149–150, Atlanta, GA, USA, 2019.
26. Dadgarpour, A., B. Zarghooni, B. S. Virdee, and T. A. Denidni, "One- and two-dimensional beam-switching antenna for millimeter-wave MIMO applications," *IEEE Transactions on Antennas and Propagation*, Vol. 64, No. 2, 564–573, Feb. 2016.